

Carbon supersaturation and clustering in bainitic ferrite at low temperature

Rosalía Rementería¹, Jonathan D. Poplawsky², Esteban Urones-Garrote³, Ricardo Domínguez-Reyes⁴,
Carlos García-Mateo¹, Francisca G. Caballero^{1*}

¹ Spanish National Center for Metallurgical Research (CENIM-CSIC), Avda Gregorio del Amo, 8,
Madrid, E-28040, Spain.

² Center for Nanophase Materials Sciences, Oak Ridge National Laboratory, PO Box 2008 MS6064,
Oak Ridge, TN 37831-6064, USA.

³ Spanish National Centre for Electron Microscopy (CNME), Facultad de Ciencias Químicas,
Universidad Complutense de Madrid, Avda. Complutense s/n, E-28040 Madrid, Spain.

⁴ Departamento de Física, Universidad Carlos III de Madrid, Avda. de la Universidad 30, E-28911
Leganés, Madrid, Spain.

Abstract: Characterisation at the nanoscale of bainite formed at low temperatures revealed that bainitic ferrite holds an amount of carbon above that expected from the paraequilibrium with austenite. These results have been explained by the increased solubility of carbon in a tetragonal ferrite lattice observed in the same nanostructures by using synchrotron radiation and X-ray diffraction analyses. The present work tries to shed new light on the source of the increased tetragonality and carbon supersaturation in bainitic ferrite formed at low temperature.

1. CARBON DISTRIBUTION IN FERRITE: THE KEY FACTOR EXPLAINING THE NATURE OF BAINITE

Bainite forms by the decomposition of austenite at intermediate temperatures which are above the martensite start (M_s) temperature but below that at which pearlite forms. Bainite grows via a displacive mechanism i.e., as plate-shaped transformation products exhibiting an invariant plane-strain surface relief effect [1]. However, a displacive mechanism does not imply that the transformation is also diffusionless [2]. For instance, Widmanstätten ferrite forms via displacive, but diffusional, growth mechanism.

The best criterion for discriminating the growth nature of bainitic ferrite in steels is whether the newly formed bainitic ferrite has the paraequilibrium (PE) carbon content or it is supersaturated in carbon. In this sense, quantitative assessments of carbon in bainitic ferrite using modern analysis techniques has become essential in the last decade to explain bainite growth mechanisms [3].

Thus, taking advantage of the extremely slow bainite reaction rates at low temperatures (below 350 °C) in high-carbon high-silicon bainitic steels [4], and atom probe tomography (APT) that offers extensive capabilities for chemical composition measurements at sub-nanometre scale, the presence of a level of carbon above that expected from PE with austenite was detected in dislocation-free bainitic ferrite [5]. Moreover, examination of APT experimental data from different steels treated between 200 and 525 °C did not show any abrupt change of the carbon content in bainitic ferrite that could indicate a difference in the bainite growth mechanism between high and low temperatures [6].

However, bainitic ferrite exhibits at the nanoscale a non-homogeneous distribution of carbon atoms in arrangements with specific compositions, i.e. Cottrell atmospheres, carbon clusters, and carbides [7]. The ferrite volume within a single platelet that is free of these carbon enriched regions is small. Proximity histograms can be compromised on the ferrite side, and a great deal of care should be taken to estimate the carbon content in regions of bainitic ferrite that are free from carbon agglomerations.

Given the relevance of assessing the actual carbon solubility in bainitic ferrite, precise and systematic carbon content values are particularly required for phase transformation theory. For this purpose, the DIAM method, used for the determination of a matrix composition and based on the distribution of isolated atoms [8], was applied in recent APT analyses [9] to determine the carbon concentration in bainitic ferrite away from dislocations, clusters, and precipitates. In this case, the

* Corresponding author. E-mail: fgc@cenim.csic.es, telephone: +34 91 553 89 00.

ferrite matrix is considered as the low-carbon regions in the material where the solute atoms are randomly distributed so that an accurate identification of all the features present in the analysed volume using proximity histograms is not needed.

Comparison of newest results with the APT values previously given in the literature [5, 6] show notable differences as Fig. 1 illustrates. However, they corroborate that in high-carbon high-silicon steels, bainitic ferrite out of carbon enriched features is supersaturated with respect to the ferrite/austenite phase boundary under PE conditions. Consistently with former results, tendencies indicate that the excess of carbon in ferrite decreases in these steels as the transformation temperature is increased. On the contrary, the bainitic ferrite matrix in medium-carbon high-silicon steels meets the carbon solubility value that is predicted by the PE with the austenite.

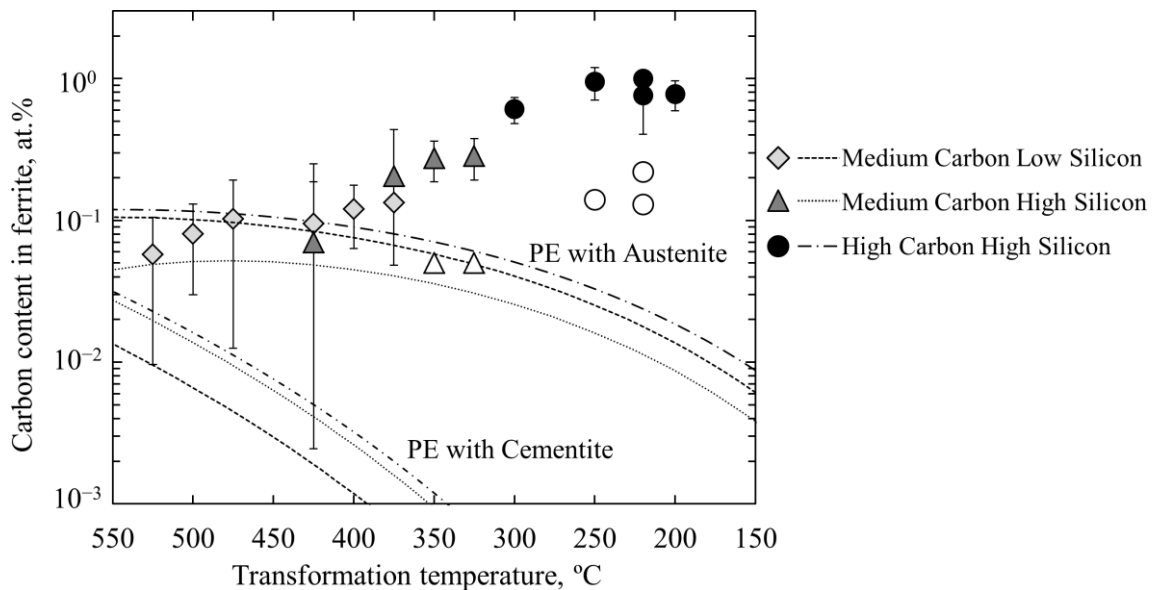


Figure 1. Comparison of APT carbon content values measured in bainitic ferrite as a function of transformation temperature in steels with different carbon and silicon contents using proximity histograms (full symbols) as reported in Refs [5] and [6] and using DIAM method (empty symbols) as reported in Ref. [9].

Beside the differences between both methods, the observed carbon in bainitic ferrite seems to persist in solid solution within bainitic ferrite following prolonged isothermal transformation at low temperatures, regardless of the competition between the rate at which carbon is partitioned from super-saturated ferrite into austenite and the rate at which carbides can precipitate from ferrite [5, 6]. The same reluctance of carbon to move from bainitic ferrite was observed when the microstructure is subjected to tempering. APT results obtained as a result of tempering of a high-carbon high-silicon steel transformed at low temperature (200°C) reported elsewhere [10], revealed that the excess of carbon in the ferrite is even evident after tempering at 500 °C for 30 min.

2. LOW TEMPERATURE BAINITE: CARBON CLUSTERING WITHIN A BCT-Fe MATRIX

The APT technique itself cannot provide the crystallographic information that might be necessary to explain this abnormal carbon content in bainitic ferrite. However, the carbon that persists in solid solution in ferrite after transformation is expected to be sufficiently Zener-ordered to produce a tetragonal or slightly orthorhombic ferrite unit cell. There are significant evidences on the tetragonality of low temperature bainitic ferrite based in *in situ* and *ex situ* synchrotron radiation experiments [11, 12]. Fig. 2 illustrates the evolution of tetragonality in bainitic ferrite obtained by Rietveld analyses of synchrotron radiation diffraction patterns during transformation at 220 and 250 °C of a high-carbon high-silicon steel as reported elsewhere [12].

Except for slight differences attributable to the error, the *c/a* ratio in the ferritic structure remains stable throughout bainite reaction at low temperature, in accordance with previous X-ray diffraction results [13]. The fact that the *c/a* ratio and the carbon content in the ferrite remains nearly constant regardless of the time after transformation could be a sign that carbon supersaturated tetragonal ferrite is the *metastable equilibrium* crystal structure resulting from the transformation.

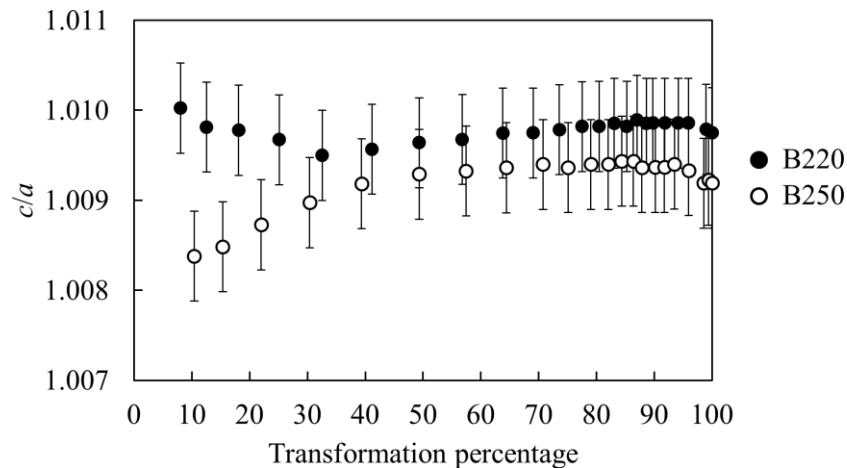


Figure 2. Evolution of the c/a ratio in bainitic ferrite during transformation at 220 °C (black points) and 250 °C (white points) in a high-carbon high-silicon steel.

It is well known that upon the displacive transformation of austenite at temperatures below that for Zener ordering, ferrite adopts a body-centred tetragonal (bct) crystal structure with the carbon atoms located at one of the three sublattices of octahedral interstices [14]. Carbon present in the parent phase is trapped in the tetragonal lattice leading to a random distribution of carbon as in virgin martensite. However, at the temperatures where carbon is mobile, the aging of the structure is unavoidable and thermal activated reactions such as carbon segregation to lattice defects, carbon atom clustering and carbide precipitation soon take place [15].

There are remarkable analogies between low temperature bainite transformation and the sequence of processes occurring during the early stages of ageing of martensite. Fig. 3 (a) presents a BF-TEM micrograph of the bainitic ferrite phase of a high-carbon high-silicon steel isothermally transformed at 250 °C, showing the characteristic *tweed-like* contrast found in naturally aged martensites. Figure 3 (b) presents the corresponding electron diffraction pattern collected inside the ferritic phase by SAED. Diffuse spikes elongating from every fundamental spot in Fig. 3 (a) arise from the short range ordering of carbon atoms, whereas satellite reflections are caused by a structural modulation with a longer period than that of the fundamental lattice. Similarly to the case of naturally aged martensite, satellite spots are attributed to the formation of a modulated structure in which carbon atom clusters are distributed randomly in periodically-spaced planes [16].

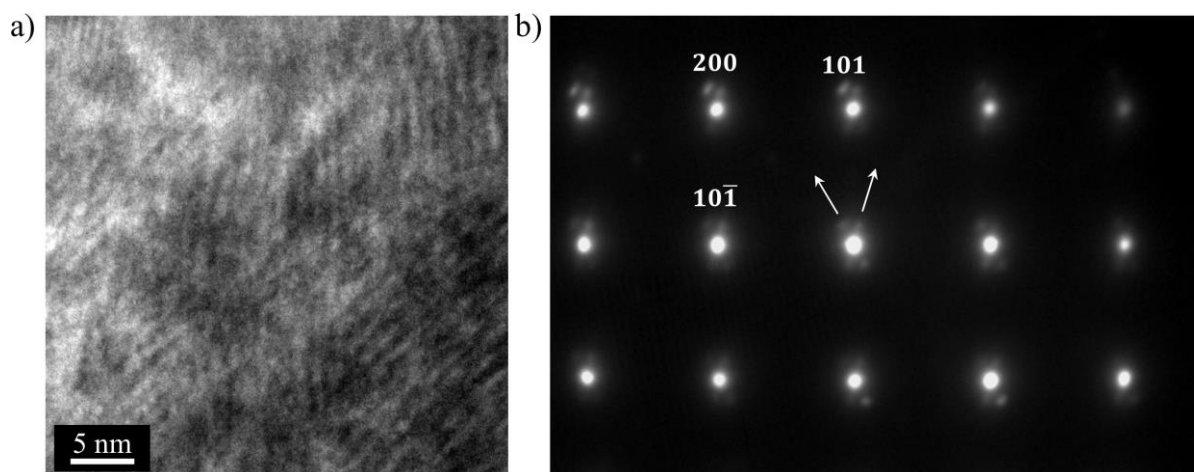


Figure 3: (a) BF-TEM image of bainitic ferrite in a high-carbon high-silicon steel isothermally transformed at 250 °C showing a *tweed-like* contrast and (b) corresponding $[100]_{\alpha}$ SAED pattern.

Similar modulated structures have also been detected in low temperature bainite by APT experiments. They are revealed as carbon clusters with a carbon content of approx. 11-12 at.% inside a carbon-depleted regions of approx. 0.2 at.% without evidence of substitutional solute partitioning such

as silicon and/or manganese. An example of a carbon atom map showing carbon clustering in bainitic ferrite is shown in Fig. 4. In general, clustering is identified by deviations from randomness in binary solid solutions. In the case of low temperature bainite, clusters are defined as a few nm thick carbon-enriched regions, sometimes with a characteristic branch-like structure, dispersed within the ferrite matrix with a carbon content close to the stoichiometric Fe_{16}C_2 compound (11.11 at.% C) [17, 18]. The composition of carbon clusters shown in Fig. 4 (c) is about 12 at.% C with a composition peak at 20 at.% C. It is remarkable that clusters in naturally aged martensite have a composition close to the stoichiometric Fe_{16}C_2 compound, although an ordered Fe_4C phase may be possible too (20 at.% C) [16]. Moreover, Fig. 4 (b) presents a proximity histogram across a carbide precipitated in a ferrite/austenite interface. As recently established [12], both cementite and η -carbide do precipitate in bainite formed at low temperature. Again, η -carbide is a metastable product unique of tempering reactions in carbon-supersaturated tetragonal matrices as those of martensite and bainitic ferrite.

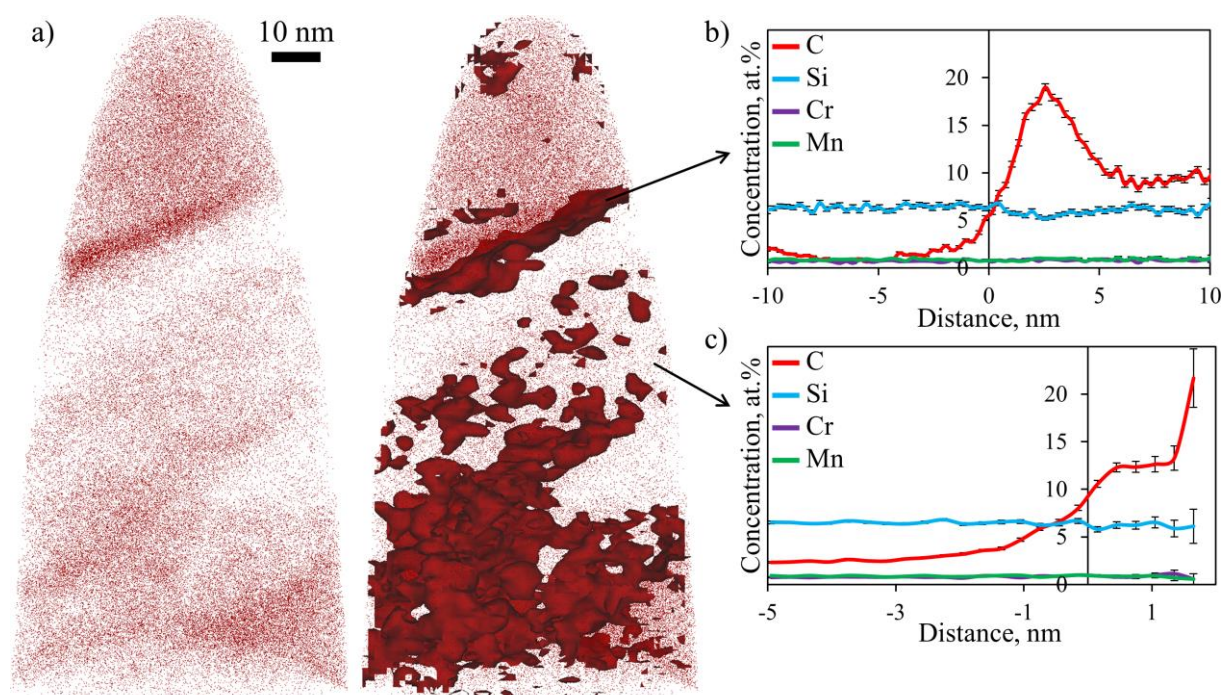


Figure 4. a) Carbon atom map and corresponding 6 at.% isoconcentration surfaces, (b) proximity histogram across a carbide precipitated in a ferrite/austenite interface and (c) proximity histogram across all the isolated clusters in the mid region indicated by an arrow in nanocrystalline bainite formed at 200 °C in a high-carbon high-silicon steel.

Earlier investigations in martensite [19-22] firmly established carbon-atom clustering as an inherent process in structure ageing. The driving force for clustering of carbon atoms was proposed to be a reduction in the lattice-distortion strain energy caused by the interstitial atoms, so that the structural modulations result from a stress-induced alignment of individual clusters. However, the possibility that carbon clustering is related to a conditional spinodal mechanism [23], where prior Zener ordering is required to produce the initial compositional instability that develops in a coherent two-phase state i.e., $\alpha \rightarrow \alpha + \alpha''$, where α'' is the stoichiometric Fe_{16}C_2 compound, cannot be ruled out.

Based on recent ab-initio density functional theory (DFT) calculations [24], clusters can be explained as strained, tetragonal regions in ferritic bainite, in which the solution enthalpy of carbon can reach large, negative values. As APT results revealed, silicon itself only has a minor influence on this phenomenon. DFT calculations showed that silicon has a repulsive effect on carbon, decreasing its solubility in both ferrite and austenite by increasing the enthalpy of solution by a comparable amount. Therefore, a big influence of silicon on the partitioning of carbon via a change in solubility is not expected after bainitic ferrite formation. Vacancies, however, improve the solubility of carbon in the Fe-Si-C system by altering the bond lengths in their nearest-neighbour surroundings. In both the

Fe–C and Fe–Si–C systems, a tetragonal distortion decreases the solution enthalpy of carbon. However, if the distortion is associated with a small superimposed volumetric strain, the effect is quite drastic, making the accumulation of carbon observed by APT plausible.

3. NATURE OF THE DEFECTS AND THEIR STABILITY IN LOW TEMPERATURE BAINITE

The presence of a high amount of intrinsic defects in structures resulting from a displacive transformation, and the subsequent formation of carbon-vacancy complexes could lead also to a carbon concentration in iron above that expected from the thermodynamic equilibrium. In this sense, assessing the nature of the defects and their stability in relation to the transformation temperature is of interest.

Positron annihilation spectroscopy (PAS) is sensitive to lattice defects and is also capable of detecting the atomic environment of positron annihilation sites [25]. Lattice defects such as vacancies, voids, solute–vacancy complexes and other open-volume defects are effective traps for thermalized positrons in metals. The annihilation radiation of a positron trapped in a defect conveys information about the nature of the defect. The positron lifetime spectra (PLS) provide information on the type and size of the defects. In addition, the Doppler broadening (CDB) of the annihilation radiation peak at 511 keV, which depends on the momentum of the electrons annihilating with the thermalized positrons, can give information about the solute surrounding the positron annihilation site [26].

The PLS results of both martensitic (M) and bainitic (B) structures obtained in a high-carbon high-silicon steel showed a lifetime of approximately 160 ps for all the studied structures, which corresponds to the lifetime of C–vacancy complexes [27]. Likewise, the shape of the CDB curves (Fig. 5) of the martensitic and bainitic structures gets away from the unity in a similar manner, implying that the defect distribution has no major chemical change on its surroundings despite the microstructure. Moreover, the CDB curves of the bainitic structures shifts towards the carbon CDB signature curve as the transformation temperature decreases. The present results indicate that a decrease in the transformation temperature results in larger amounts of carbon bound to vacancy-type defects. Lower transformation temperatures are translated into higher amounts of bainitic ferrite with also higher levels of carbon supersaturation in bainitic ferrite. Therefore, the presence of C–vacancy complexes should contribute to the carbon supersaturation levels detected in bainitic ferrite.

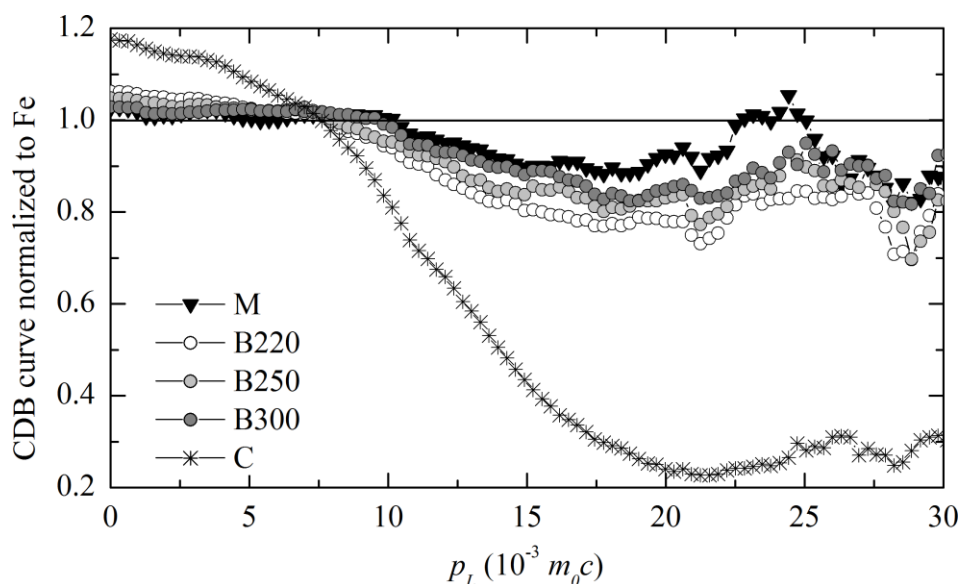


Figure 5. CDB ratio spectra for martensitic and bainitic structures obtained in a high-carbon high-silicon steel normalized by the CDB spectrum of a pure annealed Fe reference sample. B220, B250 and B300 are bainitic structures isothermally transformed at 220, 250 and 300 °C, respectively, M is the martensitic structure obtained from the same steel by rapid quenching after austenitization and C is pure carbon.

Final remarks

Given the obvious analogies of low temperature bainite transformation with the processes occurring during the ageing of martensite, it is the view of the present authors that experimental evidences shift again in favour of a supersaturated, high-velocity shear mechanism, the “martensite paradigm” [2].

Acknowledgements: This research was supported by the Spanish Ministerio de Economía y Competitividad (MINECO) in the form of a Coordinate Project (MAT2016-80875-C3-1-R); and the Research Fund for Coal and Steel under the Contract RFSR-CT- 2014-00019. APT was conducted at ORNL's Center for Nanophase Materials Sciences (CNMS), which is a U.S. DOE Office of Science User Facility.

REFERENCES

- [1] E. Swallow, H.K.D.H. Bhadeshia: *Materials Science and Technology*, 12(2) (1996), 121-125.
- [2] M. Hillert: *Scripta Materialia* 47(3) (2002), 175-180.
- [3] E.V. Pereloma: *Materials Science and Technology*, 32(2) (2016), 99-103.
- [4] F.G. Caballero, H.K.D.H. Bhadeshia: *Current Opinion in Solid State and Materials Science*, 8(3-4) (2004), 251-257.
- [5] F.G. Caballero, M.K. Miller, C. Garcia-Mateo: *Acta Materialia*, 58(7) (2010), 2338-2343.
- [6] F.G. Caballero, M.K. Miller, C. Garcia-Mateo, J. Cornide, M.J. Santofimia: *Scripta Materialia* 67(10) (2012), 846-849.
- [7] F.G. Caballero, M.K. Miller, S.S. Babu, C. Garcia-Mateo: *Acta Materialia*, 55(1) (2007), 381-390.
- [8] F.D. Geuser, W. Lefebvre: *Microscopy Research and Technique* 74(3) (2011), 257-263.
- [9] R. Rementeria, J.D. Poplawsky, M.M. Aranda, W. Guo, J.A. Jimenez, C. Garcia-Mateo, F.G. Caballero: *Acta Materialia*, 125 (2017), 359-368.
- [10] F.G. Caballero, M.K. Miller, C. Garcia-Mateo: *Metallurgical and Materials Transactions A: Physical Metallurgy and Materials Science*, 42A(12) (2011), 3660-3668.
- [11] C.N. Hulme-Smith, M.J. Peet, I. Lonardelli, A.C. Dippel, H.K.D.H. Bhadeshia: *Materials Science and Technology*, 31(2) (2015), 254-256.
- [12] R. Rementeria, J.A. Jimenez, S.Y.P. Allain, G. Geandier, J.D. Poplawsky, W. Guo, E. Urones-Garrote, C. Garcia-Mateo, F.G. Caballero: *Acta Materialia*, 133 (2017), 333-345.
- [13] C. Garcia-Mateo, J.A. Jimenez, H.W. Yen, M.K. Miller, L. Morales-Rivas, M. Kuntz, S.P. Ringer, J.R. Yang, F.G. Caballero: *Acta Materialia*, 91(0) (2015), 162-173.
- [14] C. Zener: *Transactions of the American Institute of Mining and Metallurgical Engineers*, 167 (1946), 550-595.
- [15] B.S. Lement, B.L. Averbach, M. Cohen: *Transactions of the American Society for Metals*, 46 (1954), 851-881.
- [16] K.A. Taylor, M. Cohen: *Progress in Materials Science*, 36 (1992), 151-272.
- [17] F.G. Caballero, M.K. Miller, C. Garcia-Mateo, C. Capdevila, S.S. Babu: *Acta Materialia*, 56(2) (2008), 188-199.
- [18] F.G. Caballero, M.K. Miller, C. Garcia-Mateo: *Materials Chemistry and Physics* 146(1-2) (2014), 50-57.
- [19] A.M. Sherman, G.T. Eldis, M. Cohen: *Metallurgical Transactions A*, 14(5) (1983), 995-1005.
- [20] P. Ferguson, K.H. Jack: *Scripta Metallurgica*, 18(11) (1984), 1189-1194.
- [21] Y. Hirotsu, S. Nagakura: *Transactions of the Japan Institute of Metals*, 15(2) (1974), 129-134.
- [22] Y. Hirotsu, Y.i. Itakura, K.-C. Su, S. Nagakura: *Transactions of the Japan Institute of Metals*, 17(8) (1976), 503-513.
- [23] K.A. Taylor, L. Chang, G.B. Olson, G.D.W. Smith, M. Cohen, J.B.V. Sande: *Metallurgical Transactions A*, 20(12) (1989), 2717-2737.
- [24] S. Sampath, R. Rementeria, X. Huang, J.D. Poplawsky, C. Garcia-Mateo, F.G. Caballero, R. Janisch: *Journal of Alloys and Compounds* 673 (2016), 289-294.
- [25] P. Hautojärvi, C. Corbel, Positron spectroscopy of defects in metals and semiconductors, in: A. Dupasquier, A.P.M. Jr. (Eds.) *Positron Spectroscopy of Solids*, IOS Press, Varenna on lake Como, 1993, pp. 491-532.
- [26] M.J. Puska, R.M. Nieminen: *Reviews of Modern Physics* 66(3) (1994), 841-897.
- [27] M.J. Puska, R.M. Nieminen: *Journal of Physics F: Metal Physics* 13(5) (1983), 1091.